Contemporary Mathematics
http://ojs.wiserpub.com/index.php/CM/

Research Article

The Sombor Indices of Banana Tree Graph and Fractal Tree Type Dendrimer

Thanga Rajeswari K, Manimaran A*

Department of Mathematics, School of Advanced Sciences, Vellore Institute of Technology, Vellore 632 014, Tamil Nadu, India
E-mail: manimaran.a@vit.ac.in

Received: 7 June 2024; **Revised:** 2 September 2024; **Accepted:** 3 September 2024

Abstract: Topological descriptors are graph-theoretical metrics that allow one to describe a molecular structure's underlying connectedness. Degree-based topological descriptors have been investigated widely and are associated with several chemical characteristics. The examination of graph entropy indices as a gauge for the intricacy of the underlying connection and as a means of characterizing structural attributes has also gained significance.The present study utilizes the graph-theory-based edge partition method to examine Sombor variants for the Banana Tree Graph, Fractal, and Cayley Tree Type Dendrimers. We have employed Shannon's entropy model to determine the graph-based entropy of these graphs and produced Sombor indices.

***Keywords*:** Sombor indices, banana tree graph, fractal tree, cayley tree

MSC: 05C92, 92E10, 28A80

1. Introduction

Molecular descriptors can be used to properly quantify a molecule [1, 2]. These molecular structure-derived values have several uses in chemistry [3, 4]. Their primary applications include quantitative structure-property/activity relationship (QSPR/QSAR) modeling [5–8] and simulated screening [9]. Employing topological molecular descriptors to encode molecular structural data is an effective strategy. The abundance of molecular descriptors can be attributed to their inexpensive computations and quick detection using structural features. Topological molecular descriptors are parameters that are mathematically derived from the molecular structure [10–12]. Graph invariants have proven valuable in chemistry [13–19]. Topological molecular descriptors are useful in drug discovery.

Graph variables are derived from a molecular graph using a variety of approaches. Degree, distance, and eigenvalue-based graph variables can be defined differently depending on the parameters employed. Motivated by the Euclidean metric, the author of the study "Geometric approach to degree-based topological indices: Sombor indices" has suggested novel graph variables based on vertex degree [20]. Researchers worldwide have conducted several studies employing the Sombor index in a short time [21–23]. It is a widely used index in the literature. The Sombor index has undergone many variations since its introduction [24]. Also, researchers have shown interest in studying customized versions of the Sombor index. Gutman et al. [25] introduced the Elliptic Sombor index, a new vertex-degree-based topological index

DOI: https://doi.org/10.37256/cm.5320245112

with geometric features, after previous successful work on the Sombor index and its variations. Let $\mathscr{M}$ be the molecular graph, then the parameters are specified as follows:

$$SO(\mathscr{M}) = \sum_{xy \in E} \sqrt{d^2(x) + d^2(y)} \tag{1}$$

$$SO_{red}(\mathscr{M}) = \sum_{xy \in E} \sqrt{(d(x)-1)^2 + (d(y)-1)^2} \tag{2}$$

$$SO_{inc}(\mathscr{M}) = \sum_{xy \in E} \sqrt{(d(x)+1)^2 + (d(y)+1)^2} \tag{3}$$

$$SO_{mod}(\mathscr{M}) = \sum_{xy \in E} \frac{1}{\sqrt{d^2(x) + d^2(y)}} \tag{4}$$

$$KGSO(\mathscr{M}) = \sum_{xy \in E} \left(\sqrt{d^2(x) + (d(x)+d(y)-2)^2} + \sqrt{d^2(y) + (d(x)+d(y)-2)^2} \right) \tag{5}$$

$$ESO(\mathscr{M}) = \sum_{xy \in E} (d(x)+d(y)) \left(\sqrt{d^2(x) + d^2(y)} \right) \tag{6}$$

The Sombor indices show promising predictive ability for predicting the thermodynamic characteristics of substances. The Sombor indices were examined for their ability to discriminate across various chemical tree groupings [26]. The Elliptic Sombor index (ESO) is the most effective predictor of polarizability for benzenoid hydrocarbons, followed by π-electron energy and molar refractivity, according to curvilinear regression studies [27]. When combined with entropy measurements, topological descriptors can be a more effective tool in QSAR and QSPR investigations [28–32]. Information entropy was discovered to directly correlate with the physical characteristics of fullerenes in several kinds of natural substances, including oxidation and rotational symmetry [33].

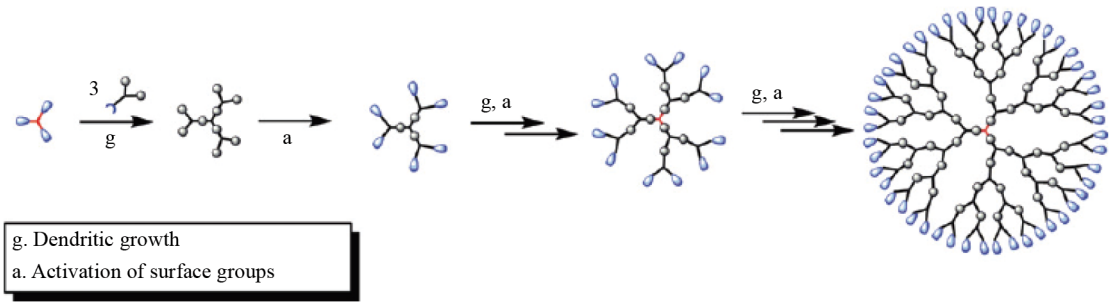

Figure 1. The method of divergent strategy for dendrimers

In the fields of pharmaceuticals, bioinformatics, and restorative science, the numerical encoding of chemical structure using topological indices is currently gaining importance. This methodology enables efficient collection, elucidation,

retrieval, analysis, and mining of mixture structures inside large-scale datasets. The organic macromolecules known as dendrimers are extremely branched, with a central core surrounded by a series of branch unit generations, or iterations [34, 35]. There are two ways to synthesize dendrimers: the divergent growth approach (Figure 1) and the convergent growth approach (Figure 2). The graphs of the banana, fractal, and cayley tree are utilized to customize the structure for the synthesis of dendrimers.

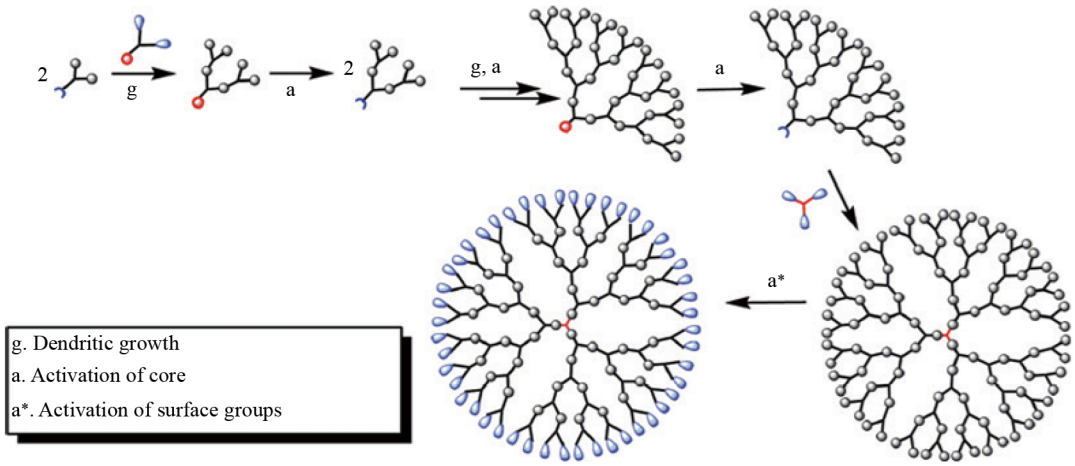

Figure 2. The method of convergent strategy for dendrimers

Additionally, we can forecast the chemical and physical characteristics of dendrimers by employing topological descriptors. In the present paper, we determined Sombor indices for Banana Tree Graph, Fractal, and Cayley Tree Type Dendrimers. Also, we computed the Sombor entropies for them.

2. Preliminaries

Entropy of a graph: To attempt to describe the complexity of graphs, graph entropy was proposed [36]. Although its introduction was intended to illustrate the intricacy of information transmission and communication, it currently finds widespread use in a variety of scientific fields, including biological networks, engineering, and physical dissipative structures [37]. The entropy evaluated using the topological descriptor T is defined as [38],

$$ENT_T(\mathscr{M}) = -\sum_{e\in E(\mathscr{M})} p_e log(p_e) \tag{7}$$

$$ENT_T(\mathscr{M}) = log(T(\mathscr{M})) - \frac{1}{T(\mathscr{M})}\sum_{e\in E(\mathscr{M})} f(e)log(f_e) \tag{8}$$

Banana Tree Graph: The banana tree is a graph constructed by linking a single leaf from each of the r replicas of s-star graphs to a unique root vertex, $r \geq 2$, $s \geq 4$ [39].

Figure 3 shows the general structure of the banana tree graph $B(r, s)$. The edge partition of $B(r, s)$ established by the degrees of terminal vertices of each edge is presented in Table 1.

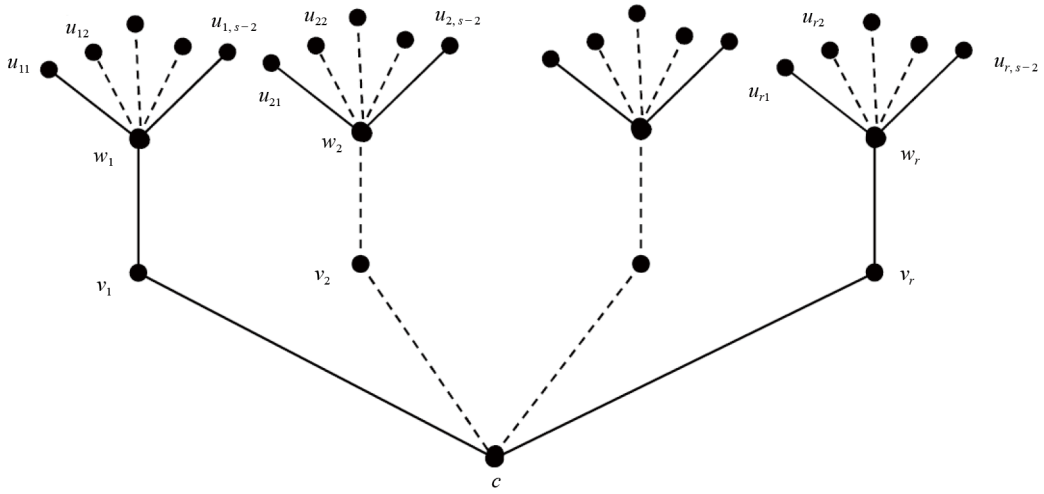

Figure 3. Banana tree $B(r, s)$

Table 1. Edge partition of $B(r, s)$ established on degrees of terminal vertices of each edge

(d_x, d_y)	Number of repitition
$(2, r)$	r
$(2, s-1)$	r
$(1, s-1)$	$r(s-2)$

Fractal Tree Type Dendrimer: Fractal geometry is the study of geometric shapes that systematically form smaller curves or patterns. There is a rough fractal structure to the way a tree's stem divides into progressively tiny branches and limbs. Numerous additional fractal examples exist, such as the Von Koch snowflake, Angelica flowerhead, Lotus white flower, ferns, and lightning bolt.

The fractal tree dendrimers presented here are referred to as F_ι, where $\iota \geq 0$ denotes the number of repetitions. F_0 has a single edge linking two vertices. F_ι is generated by completing two steps for each continuous edge in $F_{\iota-1}$. Initially, a path consisting of three connections with identical terminals must be generated. In the subsequent step, generate η additional vertices for each of those two intermediate vertices in the path, then connect them to the adjacent vertices.

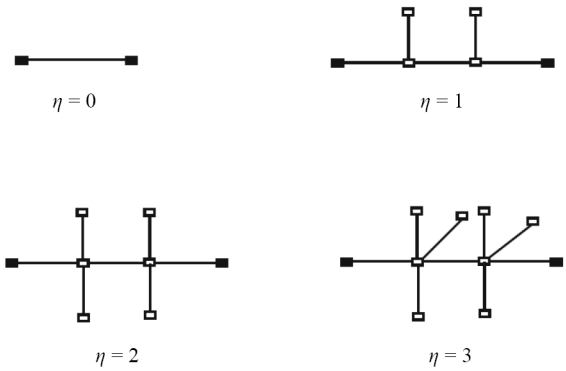

Figure 4. Building fractal trees for $\eta = 0, 1, 2, 3$

Figure 4 exhibits the configuration for various values of η. In Figure 5(a) and 5(b), F_3 for $\eta = 2$ and F_4 for $\eta = 3$ are generated, respectively. Employing edge partition methodology and graph theoretic approaches, we initially construct the aforementioned sombor indices for Fractal Tree Dendrimer. F_ι has $42\iota\eta - 28\eta + 14\iota - 8$ pendent vertices. $7\iota - 5$ are the vertices with degree 4, and the vertices with $\eta + 2$ are $42\iota - 28$ numerically. With respect to the degree of the end vertices, there are three distinct kinds of edges in the edge set of F_ι in Table 2.

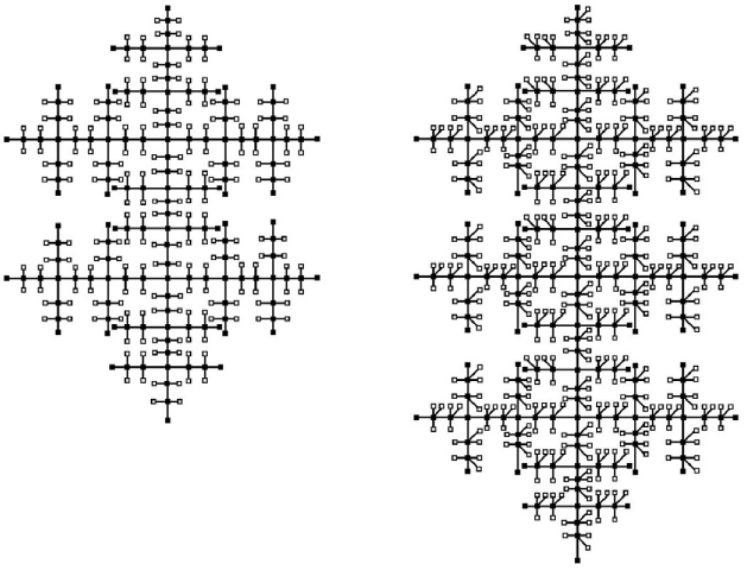

(a) (b)

Figure 5. (a) F_3 for $\eta = 2$ is generated. (b) F_4 for $\eta = 3$ is generated

Table 2. Edge partition of F_ι established on degrees of terminal vertices of each edge

$(d_u,\ d_v)$	No. of repetition
$(1,\ \eta+2)$	$42\iota\eta - 28\eta + 14\iota - 8$
$(4,\ \eta+2)$	$28\iota - 20$
$(\eta+2,\ \eta+2)$	$21\eta - 14$

Cayley Tree Type Dendrimer: Every non-leaf graph vertex in a Cayley tree has a certain number of branches. With $\nu + 1$ nodes, the star graph is a unique ν-cayley tree. Dendrimers include the Cayley tree, commonly referred to as the Bathe lattice. We utilize an iterative technique to build the Cayley tree $C(\nu,\ \kappa)$, where $\nu \geq 3$ and $\kappa \geq 0$. The nodes in this instance are represented by ν. There is simply a single central vertex in $C(\nu,\ 0)$. Generating ν nodes and connecting them to the center vertex using an edge yields $C(\nu,\ 1)$. By constructing $\kappa - 1$ nodes and connecting them to each of the vertices with degree 1 of $C(\nu,\ \kappa)$, $C(\nu,\ \kappa)$ is derived from $C(\nu,\ \kappa - 1)$ in Figure 6.

The number of vertices with degree 1 and degree ν are $\nu(\nu-1)^{(\kappa-1)}$ and $2\sum_{i=1}^{\kappa}(\nu-1)^{(i-1)} - (\nu-1)^{(\kappa-1)}$, respectively. The cardinality of vertex and edge sets are $2\sum_{i=1}^{\kappa}(\nu-1)^{(i-1)} - (\nu-1)^{\kappa}$ and $\nu\sum_{i=1}^{\kappa}(\nu-1)^{(i-1)}$, respectively.

There are two distinct kinds of edges in the edge set of $C(\nu,\ \kappa)$, depending on the degree of the end vertices. The edge partition of $C(\nu,\ \kappa)$ is displayed in Table 3.

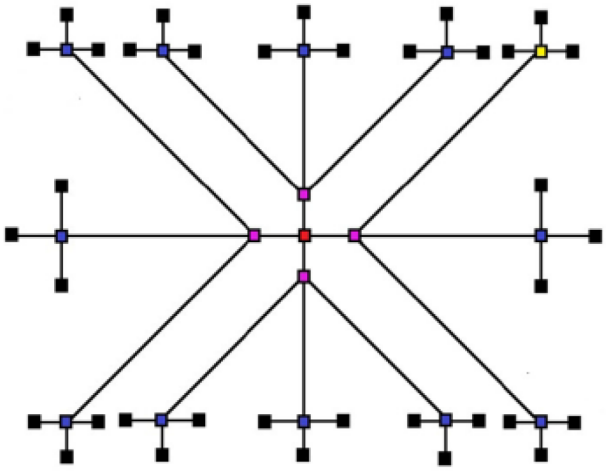

Figure 6. The cayley tree type dendrimer for $C(4, 3)$

Table 3. Edge partition of $C(\nu, \kappa)$ established on degrees of terminal vertices of each edge

(d_u, d_v)	Frequency
$(1, \nu)$	$\nu(\nu-1)^{\kappa-1}$
(ν, ν)	$\nu\sum_{i=1}^{\kappa}(\nu-1)^{i-1} - \nu(\nu-1)^{\kappa-1}$

3. Results and discussion

Theorem 1 For the Banana Tree Graph $B(r, s)$, the values of Sombor indices are

1. $SO(B(r, s)) = r\left(\sqrt{r^2+4}+\sqrt{s^2-2s+5}+(s-2)\sqrt{s^2-2s+2}\right)$.
2. $SO_{red}(B(r, s)) = r\left(\sqrt{r^2-2r+2}+\sqrt{s^2-4s+5}+(s-2)^2\right)$.
3. $SO_{inc}(B(r, s)) = r\left(\sqrt{r^2+2r+10}+\sqrt{s^2+9}+(s-2)\sqrt{s^2+4}\right)$.
4. $SO_{mod}(B(r, s)) = r\left(\frac{1}{\sqrt{r^2+4}}+\frac{1}{\sqrt{s^2-2s+5}}+\frac{s-2}{\sqrt{s^2-2s+2}}\right)$.
5. $KGSO(B(r, s)) = r\left(\sqrt{r^2+4}+\sqrt{2}(r^2+s-1)+\sqrt{s^2-2s+5}+(s-2)(\sqrt{s^2-4s+5}+\sqrt{2s^2-6s+5})\right)$.
6. $ESO(B(r, s)) = r\left((r+2)\sqrt{r^2+4}+(s+1)\sqrt{s^2-2s+5}+s(s-2)\sqrt{s^2-2s+2}\right)$.

Result 1 For the Banana Tree Graph $B(r, s)$, the values of Sombor entropies are

1. $ENT_{SO}(B) = log(SO) - \frac{1}{SO}\Big((r\sqrt{r^2+4}log(\sqrt{r^2+4}))$
$+(r\sqrt{s^2-2s+5}log(\sqrt{s^2-2s+5}))+(r(s-2)\sqrt{s^2-2s+2}log(\sqrt{s^2-2s+2}))\Big)$.
2. $ENT_{SO_{red}}(B) = log(SO_{red}) - \frac{1}{SO_{red}}\Big((r\sqrt{r^2-2r+2}log(\sqrt{r^2-2r+2}))+(r\sqrt{s^2-4s+5}log(\sqrt{s^2-4s+5}))$
$+(r(s-2)^2log(s-2))\Big)$.

3. $ENT_{SO_{inc}}(B) = log(SO_{inc}) - \frac{1}{SO_{inc}}\Big((r\sqrt{r^2+2r+10}log(\sqrt{r^2+2r+10}))$
$+(r\sqrt{s^2+9}log(\sqrt{s^2+9})) + (r(s-2)\sqrt{s^2+4}log(\sqrt{s^2+4}))\Big)$.

4. $ENT_{SO_{mod}}(B) = log(SO_{mod}) - \frac{1}{SO_{mod}}\left(\left(\frac{r}{\sqrt{r^2+4}}log\left(\frac{1}{\sqrt{r^2+4}}\right)\right) + \left(\frac{r}{\sqrt{s^2-2s+5}}log\left(\frac{1}{\sqrt{s^2-2s+5}}\right)\right)\right.$
$\left. + \left(\frac{r(s-2)}{\sqrt{s^2-2s+2}}log\left(\frac{r(s-2)}{\sqrt{s^2-2s+2}}\right)\right)\right)$.

5. $ENT_{KGSO}(B) = log(KGSO) - \frac{1}{KGSO}\Big(((r(\sqrt{r^2+4}+r\sqrt{2}))log(\sqrt{r^2+4}+r\sqrt{2}))$
$+((r(\sqrt{s^2-2s+5}+(s-1)\sqrt{2}))log(\sqrt{s^2-2s+5}+(s-1)\sqrt{2}))$
$+(r(s-2)(\sqrt{s^2-4s+5}+\sqrt{2s^2-6s+5})log(\sqrt{s^2-4s+5}+\sqrt{2s^2-6s+5}))\Big)$.

6. $ENT_{ESO}(B) = logESO - \frac{1}{ESO}\Big((r(r+2)\sqrt{r^2+4}log((r+2)\sqrt{r^2+4}))$
$+(r(s+1)\sqrt{s^2-2s+5}log((s+1)\sqrt{s^2-2s+5})) + (rs(s-2)\sqrt{s^2-2s+2}log(s\sqrt{s^2-2s+2}))\Big)$.

Table 4. Numerical values of Sombor indices for $B(r, s)$

$B(r, s)$	$SO(B)$	$SO_{red}(B)$	$SO_{inc}(B)$	$SO_{mod}(B)$	$KGSO(B)$	$ESO(B)$
(2, 4)	25.5171	15.3006	36.3738	2.5267	50.3766	109.2794
(2, 5)	39.3398	27.1530	52.4582	2.6095	80.5454	199.9862
(3, 4)	40.6070	25.4164	56.8328	3.5615	82.1389	184.0612
(3, 5)	61.3410	43.1950	80.9593	3.6857	127.3920	320.1215
(4, 4)	57.6090	37.5934	79.1009	4.5336	118.6417	280.6352
(4, 5)	85.2544	61.2982	111.2696	4.6993	178.9793	462.0489
(5, 4)	76.5764	51.7959	103.2624	5.4775	159.9383	405.1107
(5, 5)	111.1331	81.4269	143.4733	5.6845	235.3603	631.8778

Table 5. Numerical values of Sombor entropies for $B(r, s)$

$B(r, s)$	$ENT_{SO}(B)$	$ENT_{SO_{red}}(B)$	$ENT_{SO_{inc}}(B)$	$ENT_{SO_{mod}}(B)$	$ENT_{KGSO}(B)$	$ENT_{ESO}(B)$
(2, 4)	2.0757	2.0662	1.3410	2.0758	2.1670	2.0625
(2, 5)	2.2913	2.2689	1.2602	2.2876	2.3474	2.2694
(3, 4)	2.4828	2.4834	1.7762	2.4828	2.6870	2.4695
(3, 5)	2.7057	2.7012	1.6989	2.7056	2.8407	2.6990
(4, 4)	2.7619	2.7530	2.0889	2.7633	3.0762	2.7208
(4, 5)	2.9949	2.9954	2.0172	2.9949	3.2096	2.9872
(5, 4)	2.9689	2.9421	2.3320	2.9754	3.3885	2.8797
(5, 5)	3.2131	3.2104	2.2671	3.2140	3.5064	3.1867

The Tables 4, 5 and Figures 7, 8 present the results both graphically and quantitatively. These computations show that the entropy and index values of $B(r,\ s)$ increased when r, s increased. Additionally, compared to other descriptors, the elliptic sombor index and the KGSO entropy develop faster when the structure of $B(r,\ s)$ develops, while the increased sombor entropy rises leisurely.

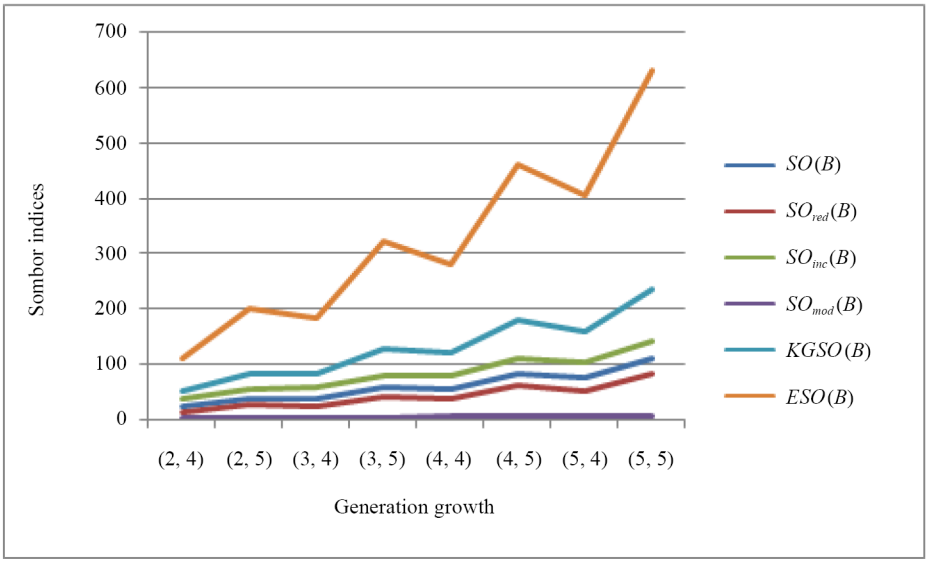

Figure 7. Graphical representation of Sombor indices of $B(r,\ s)$

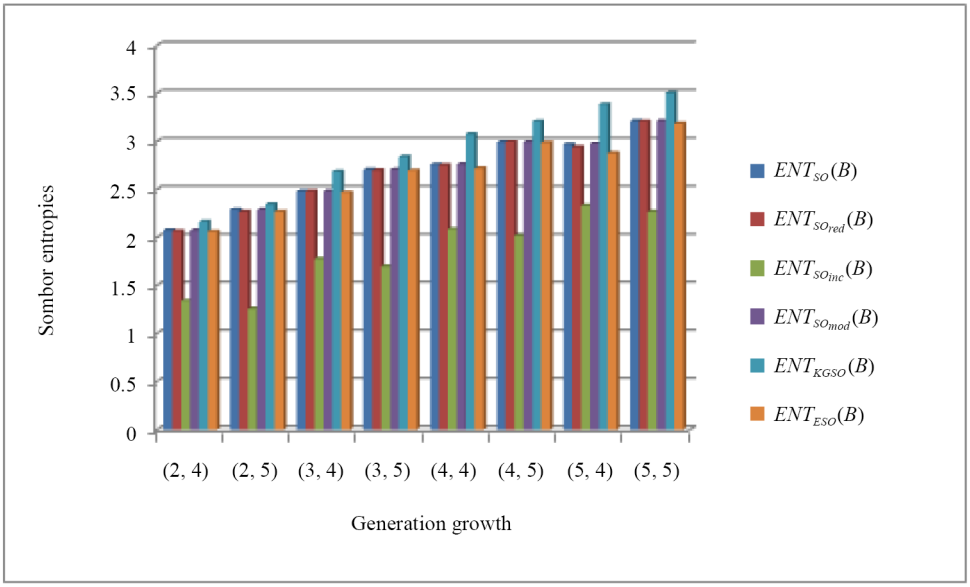

Figure 8. Graphical representation of Sombor entropies of $B(r,\ s)$

Theorem 2 For the fractal tree type dendrimer F_ι, the Sombor indices are

1. $SO(F_\iota) = 4(7\iota-5)\sqrt{\eta(\eta+4)+20}+(14\eta(3\iota-2)+14\iota-8)\sqrt{(\eta+2)^2+1}+7\sqrt{2}(\eta+2)(3\eta-2)$.

2. $SO_{red}(F_\iota) = (\eta+1)[7\sqrt{2}(3\eta-2)+2(7\eta(3\iota-2)+7\iota-4)]+4(7\iota-5)\sqrt{\eta^2}+2\eta+10.$
3. $SO_{inc}(F_\iota) = 2(7\eta(3\iota-2)+7\iota-4)\sqrt{\eta^2+6\eta+13}+4(7\iota-5)\sqrt{\eta^2+6\eta+34}+7\sqrt{2}(\eta+3)(3\eta-2).$
4. $SO_{mod}(F_\iota) = \dfrac{4(7\iota-5)}{\sqrt{\eta^2+4\eta+20}}+\dfrac{2(7\eta(3\iota-2)+7\iota-4)}{\sqrt{\eta^2+4\eta+5}}+\dfrac{7(3\eta-2)}{\sqrt{2}(\eta+2)}.$
5. $KGSO(F_\iota) = (42\iota\eta-28\eta+14\iota-8)(\sqrt{\eta^2+2\eta+2}+\sqrt{2\eta^2+6\eta+5})+4(7\iota-5)$
$(\sqrt{\eta+8\eta+32}+\sqrt{2\eta^2+12\eta+20})+14(3\eta-2)\sqrt{5\eta^2+16\eta+8}.$
6. $ESO(F_\iota) = 2(\eta+3)(7\eta(3\iota-2)+7\iota-4)\sqrt{\eta^2+4\eta+5}$
$+4(7\iota-5)(\eta+6)\sqrt{\eta^2+4\eta+20}+7\sqrt{2}(3\eta-2)(2\eta+4)(\eta+2).$

Table 6. Numerical values of Sombor indices for $F(\iota,\ \eta)$

$F(\iota,\ \eta)$	$SO(F)$	$SO_{red}(F)$	$SO_{inc}(F)$	$SO_{mod}(F)$	$KGSO(F)$	$ESO(F)$
(1, 1)	132.944	88.643	180.266	9.575	290.097	711.173
(2, 2)	906.289	667.529	1,163.400	43.328	2,030.400	5,617.600
(3, 3)	2,428.800	1,909.200	2,990.100	81.251	5,504.000	17,188.000
(4, 4)	4,955.700	4,071.400	5,910.700	120.962	11,318.000	39,650.000
(5, 5)	8,741.400	7,409.100	10,177.000	161.538	20,080.000	78,239.000
(6, 6)	14,039.000	12,176.000	16,041.000	202.5757	32,400.000	139,190.000

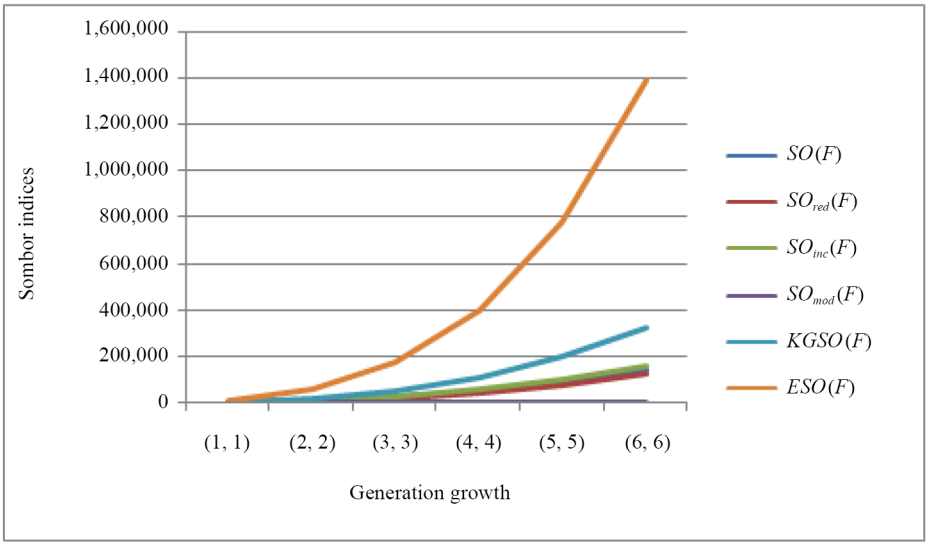

Figure 9. Graphical representation of Sombor entropies of F_ι

Result 2 For the fractal tree type dendrimer F_ι, the Sombor entropies are

1. $ENT_{SO}(F_\iota) = log(SO(F_\iota)) - \dfrac{1}{SO(F_\iota)}\Big[(42\iota\eta-28\eta+14\iota-8)\sqrt{(\eta+2)^2+1}log(\sqrt{(\eta+2)^2+1})$
$+4(7\iota-5)\sqrt{\eta(\eta+4)+20}log(\sqrt{\eta(\eta+4)+20})+7\sqrt{2}(3\eta-2)(\eta+2)log(\sqrt{2}(\eta+2))\Big].$

2. $ENT_{SO_{red}}(F_\iota) = log(SO_{red}(F_\iota)) - \frac{1}{SO_{red}(F_\iota)}\Big[(42\iota\eta - 28\eta + 14\iota - 8)(\eta+1)log(\eta+1)$
$+4(7\iota-5)\sqrt{\eta^2+2\eta+10}log(\sqrt{\eta^2+2\eta+10}) + 7(3\eta-2)\sqrt{2}(\eta+1)log(\sqrt{2}(\eta+1))\Big]$.

3. $ENT_{SO_{inc}}(F_\iota) = log(SO_{inc}(F_\iota)) - \frac{1}{SO_{inc}(F_\iota)}\Big[(42\iota\eta - 28\eta + 14\iota - 8)\sqrt{\eta^2+6\eta+13}$
$log(\sqrt{\eta^2+6\eta+13}) + 4(7\iota-5)\sqrt{\eta^2+6\eta+34}log(\sqrt{\eta^2+6\eta+34})$
$+7\sqrt{2}(\eta+3)(3\eta-2)log(\sqrt{2}(\eta+3))\Big]$.

4. $ENT_{SO_{mod}}(F_\iota) = log(SO_{mod}(F_\iota)) - \frac{1}{SO_{mod}(F_\iota)}\left(\frac{42\iota\eta - 28\eta + 14\iota - 8}{\sqrt{\eta^2+4\eta+5}}log\left(\frac{1}{\sqrt{\eta^2+4\eta+5}}\right)\right.$
$\left. + \frac{7(3\eta-2)}{\sqrt{2}(\eta+2)}log\left(\frac{1}{\sqrt{2}(\eta+2)}\right) + \frac{4(7\iota-5)}{\sqrt{\eta^2+4\eta+20}}log\left(\frac{1}{\sqrt{\eta^2+4\eta+20}}\right)\right)$.

5. $ENT_{KGSO}(F_\iota) = log(KGSO(F_\iota)) - \frac{1}{KGSO(F_\iota)}\Big[(42\iota\eta - 28\eta + 14\iota - 8)(\sqrt{\eta^2+2\eta+2}+\sqrt{2\eta^2+6\eta+5})$
$log(\sqrt{\eta^2+2\eta+2}+\sqrt{2\eta^2+6\eta+5}) + 4(7\iota-5)(\sqrt{\eta^2+8\eta+32}+\sqrt{2\eta^2}+12\eta+20)$
$log(\sqrt{\eta^2+8\eta+32}+\sqrt{2\eta^2+12\eta+20}) + 14(3\eta-2)\sqrt{5\eta^2+16\eta+8}$
$log(2\sqrt{5\eta^2+16\eta+8})\Big]$.

6. $ENT_{ESO}(F_\iota) = log(ESO(F_\iota)) - \frac{1}{ESO(F_\iota)}\Big[(42\iota\eta - 28\eta + 14\eta - 8)(\eta+3)\sqrt{\eta^2+4\eta+5}$
$log((\eta+3)\sqrt{\eta^2+4\eta+5}) + 4(7\iota-5)(\eta+6)\sqrt{\eta^2+4\eta+20}log((\eta+6)\sqrt{\eta^2+4\eta+20})$
$+7\sqrt{2}(3\eta-2)(2\eta+4)(\eta+2)log((2\eta+4)\sqrt{2}(\eta+2)\Big]$.

Table 7. Numerical values of Sombor entropies for $F(\iota,\ \eta)$

$F(\iota,\ \eta)$	$ENT_{SO}(F)$	$ENT_{SO_{red}}(F)$	$ENT_{SO_{inc}}(F)$	$ENT_{SO_{mod}}(F)$	$ENT_{KGSO}(F)$	$ENT_{ESO}(F)$
(1, 1)	3.5351	3.5223	3.5430	3.5376	3.4968	3.4534
(2, 2)	5.2664	5.2640	5.2695	5.2680	5.2340	5.2022
(3, 3)	6.0810	6.0804	6.0825	6.0825	6.0546	6.0264
(4, 4)	6.6402	6.6399	6.6410	6.6416	6.6184	6.5916
(5, 5)	7.0706	7.0705	7.0712	7.0720	7.0524	7.0265
(6, 6)	7.4221	7.4219	7.4224	7.4233	7.4064	7.3814

The findings are shown both visually and statistically in the Tables 6, 7 and Figures 9, 10. The results of this analysis demonstrate that when i climbed, so did the entropy and index values of F_ι. Moreover, as the structure of F_ι grows, ESO and ENT_{SO} develop more quickly than other descriptors.

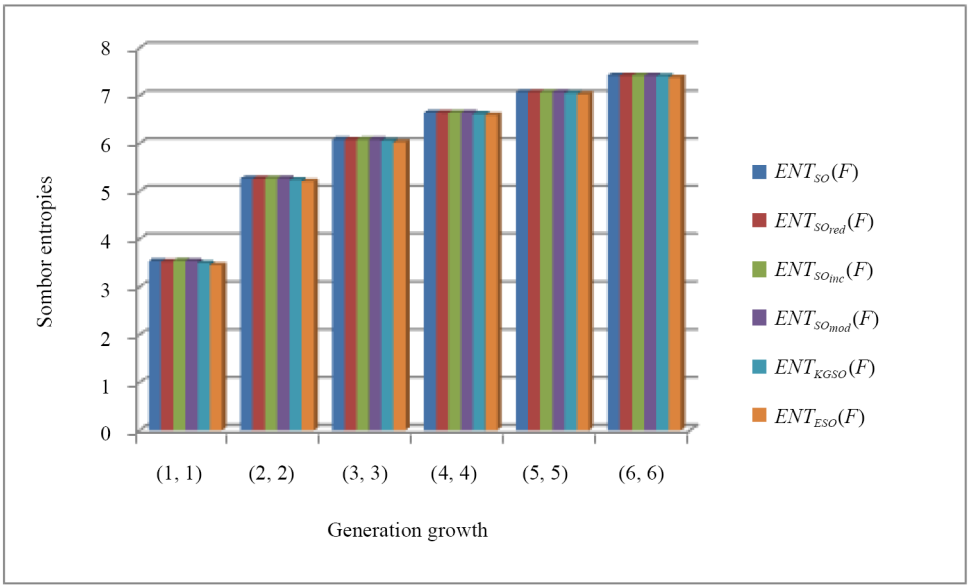

Figure 10. Graphical representation of Sombor indices of $C(\nu,\ \kappa)$

Theorem 3 For the Cayley Tree Type Dendrimer $C(\nu,\ \kappa)$, the sombor indices are

1. $SO(C(\nu,\ \kappa)) = \nu(\nu-1)^{\kappa-1}(\sqrt{\nu^2+1}-\sqrt{2}\nu)+\sqrt{2}\nu^2\sum_{i=1}^{\kappa}(\nu-1)^{i-1}.$
2. $SO_{red}(C(\nu,\ \kappa)) = \nu(\nu-1)^{\kappa}(1-\nu\sqrt{2})+\sqrt{2}\nu\sum_{i=1}^{\kappa}(\nu-1)^{i}.$
3. $SO_{inc}(C(\nu,\ \kappa)) = \nu(\nu-1)^{\kappa-1}(\sqrt{\nu^2+2\nu+5}-\sqrt{2}(\nu+1))+\sqrt{2}\nu\sum_{i=1}^{\kappa}(\nu-1)^{i-1}(\nu+1).$
4. $SO_{mod}(C(\nu,\ \kappa)) = \nu(\nu-1)^{\kappa-1}\left(\frac{1}{\sqrt{\nu^2+1}}-\frac{1}{\sqrt{2}\nu}\right)+\frac{1}{\sqrt{2}}\sum_{i=1}^{\kappa}(\nu-1)^{i-1}.$
5. $KGSO(C(\nu,\ \kappa)) = \nu(\nu-1)^{\kappa-1}\left[\sqrt{\nu^2-2\nu+2}+\sqrt{2\nu^2-2\nu+1}-2\sqrt{\nu^2+4(\nu-1)^2}\right]$
$+2\nu\sqrt{\nu^2+4(\nu-1)^2}\sum_{n=1}^{\kappa}(\nu-1)^{i-1}.$
6. $ESO(C(\nu,\ \kappa)) = \nu(\nu-1)^{\kappa-1}\left[(\nu+1)\sqrt{\nu^2+1}-2\sqrt{2}\nu^2\right]+2\sqrt{2}\nu^3\sum_{n=1}^{\kappa}(\nu-1)^{i-1}.$

Table 8. Numerical values of Sombor indices for $C(\nu,\ \kappa)$

$C(\nu,\ \kappa)$	$SO(C)$	$SO_{red}(C)$	$SO_{inc}(C)$	$SO_{mod}(C)$	$KGSO(C)$	$ESO(C)$
(3, 1)	9.4868	6.000	13.416	0.9487	17.525	37.947
(4, 2)	72.1047	52.971	92.906	3.6175	155.640	428.410
(5, 3)	584.6983	461.420	718.100	19.225	1,313.800	4,215.300
(6, 4)	6,140.300	5,065.200	7,301.400	145.220	14,020.000	50,874.000
(7, 5)	82,097.000	69,816.000	95,321.000	1,466.100	189,200.000	764,460.000
(8, 6)	1,337,500.000	1,163,000.000	1,524,800.000	18,658.000	3,102,700.000	13,812,000.000

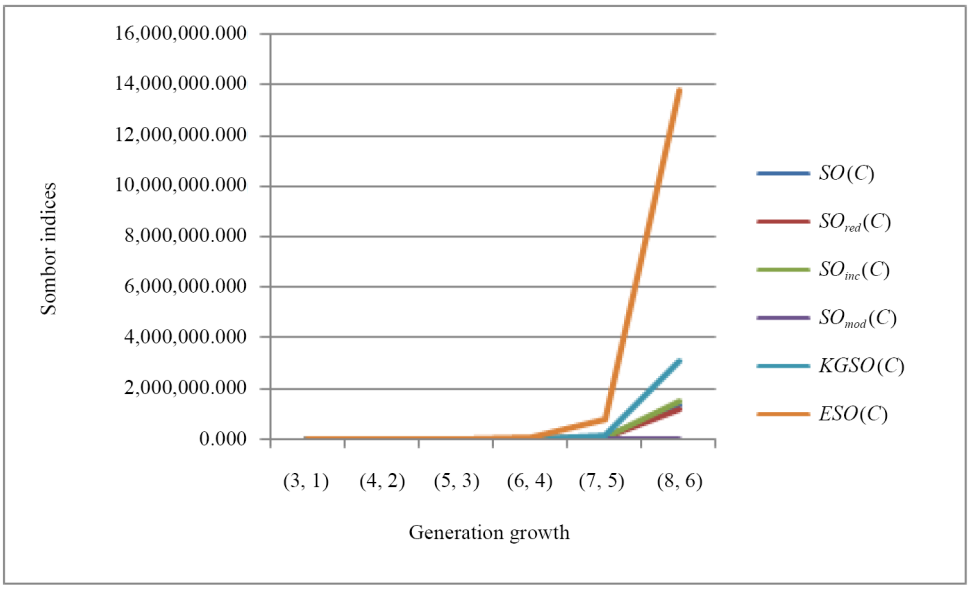

Figure 11. Graphical representation of Sombor indices of $C(\nu,\ \kappa)$

Result 3 For the Cayley Tree Type Dendrimer, the sombor entropies are

1. $$ENT_{SO}(C(\nu,\ \kappa)) = log(SO(C(\nu,\ \kappa))) - \frac{1}{SO(C(\nu,\ \kappa))}\Bigg[\nu(\nu-1)^{\kappa-1} (\sqrt{\nu^2+1}log\sqrt{\nu^2+1} - \nu\sqrt{2}log(\nu\sqrt{2})) + \sqrt{2}\nu^2 log(\nu\sqrt{2})\sum_{i=1}^{\kappa}(\nu-1)^{i-1}\Bigg].$$

2. $$ENT_{SO_{red}}(C(\nu,\ \kappa)) = log(SO_{red}(C(\nu,\ \kappa))) - \frac{1}{SO_{red}(C(\nu,\ \kappa))}\Bigg(\nu(\nu-1)^{\kappa}[log(\nu-1) - \sqrt{2}log(\sqrt{2}(\nu-1))]. + \sqrt{2}\nu(\nu-1)log(\sqrt{2}(\nu-1))\sum_{i=1}^{\kappa}(\nu-1)^{i-1}\Bigg).$$

3. $$ENT_{SO_{inc}}(C(\nu,\ \kappa)) = log(SO_{inc}(C(\nu,\ \kappa))) - \frac{1}{SO_{inc}(C(\nu,\ \kappa))}\Bigg[\nu(\nu-1)^{\kappa-1}[\sqrt{\nu^2+2\nu+5}log(\sqrt{\nu^2+2\nu+5}) - \sqrt{2}(\nu+1)log(\sqrt{2}(\nu+1))] + \sqrt{2}\nu(\nu+1)log(\sqrt{2}(\nu+1))\sum_{i=1}^{\kappa}(\nu-1)^{i-1}\Bigg].$$

4. $$ENT_{SO_{mod}}(C(\nu,\ \kappa)) = log(SO_{mod}(C(\nu,\ \kappa))) - \frac{1}{SO_{mod}(C(\nu,\ \kappa))}\Bigg[\nu(\nu-1)^{\kappa-1}\Bigg[\frac{1}{\sqrt{\nu^2+1}}log\Bigg(\frac{1}{\sqrt{\nu^2+1}}\Bigg) - \frac{1}{\sqrt{2}\nu}log\Bigg(\frac{1}{\sqrt{2}\nu}\Bigg)\Bigg] + \frac{1}{\sqrt{2}}log\Bigg(\frac{1}{\sqrt{2}\nu}\Bigg)\sum_{i=1}^{\kappa}(\nu-1)^{i-1}\Bigg].$$

5. $$ENT_{KGSO}(C(\nu,\ \kappa)) = log(KGSO(C(\nu,\ \kappa))) - \frac{1}{KGSO(C(\nu,\ \kappa))}\Bigg[\nu(\nu-1)^{\kappa-1}[(\sqrt{(\nu-1)^2+1} + \sqrt{(\nu-1)^2+\nu^2})log(\sqrt{(\nu-1)^2+1} + \sqrt{(\nu-1)^2+\nu^2}) - (2\sqrt{\nu^2+4(\nu-1)^2} log(2\sqrt{\nu^2+4(\nu-1)^2}))] + 2\nu\sqrt{\nu^2+4(\nu-1)^2}log(2\sqrt{\nu^2+4(\nu-1)^2})\sum_{i=1}^{\kappa}(\nu-1)^{i-1}\Bigg].$$

6. $$ENT_{ESO}(C(\nu,\ \kappa)) = log(ESO(C(\nu,\ \kappa))) - \frac{1}{ESO(C(\nu,\ \kappa))}\Bigg[\nu(\nu-1)^{\kappa-1}[(\nu+1)\sqrt{\nu^2+1}log((\nu+1)\sqrt{\nu^2+1}) - 2\sqrt{2}\nu^2 log(2\sqrt{2}\nu^2)] + 2\sqrt{2}\nu^3 log(2\sqrt{2}\nu^2)\sum_{i=1}^{\kappa}(\nu-1)^{i-1}\Bigg].$$

Table 9. Numerical values of Sombor entropies for $C(\nu, \kappa)$

$C(\nu, \kappa)$	$ENT_{SO}(C)$	$ENT_{SO_{red}}(C)$	$ENT_{SO_{inc}}(C)$	$ENT_{SO_{mod}}(C)$	$ENT_{KGSO}(C)$	$ENT_{ESO}(C)$
(3, 1)	1.0986	1.0986	1.0986	1.0986	1.0986	1.0986
(4, 2)	2.7623	2.7601	2.7650	2.7642	2.7370	2.7018
(5, 3)	4.6432	4.6418	4.6453	4.6454	4.6173	4.5743
(6, 4)	6.8316	6.8307	6.8332	6.8340	6.8073	6.7612
(7, 5)	9.2861	9.2855	9.2872	9.2884	9.2637	9.2169
(8, 6)	11.9550	11.9550	11.9560	11.9570	11.9340	11.8880

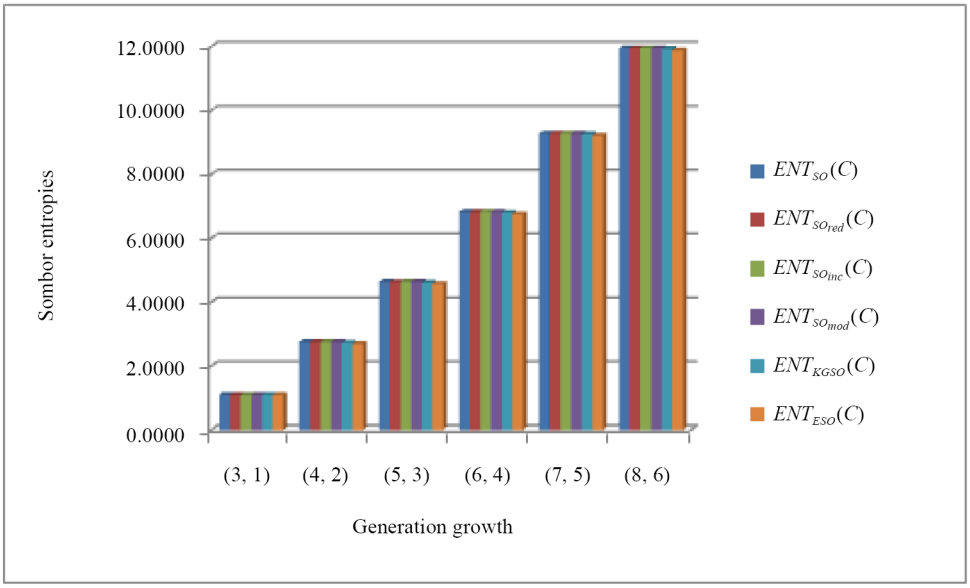

Figure 12. Graphical representation of Sombor entropies of $C(\nu, \kappa)$

The outcomes are presented both graphically and statistically in the Tables 8, 9 and Figures 11, 12. The above computations indicate that when ν, κ grew, so did the entropy and index values of $C(\nu, \kappa)$. Also, as the layout of $C(\nu, \kappa)$ grows, ESO and ENT_{SO} increase rapidly than other descriptors.

4. Application

The banana tree graph can help visualize the branching patterns of dendrons, where the central vertex represents the core of the dendron from which linear arms extend. Insights from the banana tree graph can inform the design and synthesis of dendrons with specific branching structures, allowing researchers to control the number and length of the arms to achieve desired properties. In drug development, our established topological indices and the entropy measurements of the banana tree graph can potentially be useful in predicting the physicochemical properties, thermodynamic features, molar refractivity, optical, and mechanical properties of the dendrons.

Fractal trees can serve as a model for dendrimer growth, where each level of the fractal represents a new generation of dendrimer branches. This can aid in visualizing and designing dendrimers with specific branching patterns. Fractal trees

can help in analyzing the branching patterns of dendrimers, which is crucial for understanding their structure-property relationships and optimizing their synthesis pathways. By mapping functional groups onto the branches of a fractal tree, researchers can visualize and optimize the distribution of functional groups on the dendrimer surface, influencing its reactivity and solubility. Understanding dendrimer growth as a fractal process can help in controlling the size, shape, and uniformity of dendrimers, leading to more efficient synthesis methods. Insights from fractal tree models can help minimize defects in dendrimer structures, ensuring a higher degree of structural perfection. Our defined sombor indices for fractal trees can be beneficial in measuring complexity, property prediction, and synthesis optimization of dendrimers.

The Cayley tree's hierarchical, branching structure is similar to that of dendrimers, which grow from a central core outward in successive generations. This makes the Cayley tree a natural model for representing dendrimer architecture. It helps in visualizing and understanding the branching patterns and connectivity within dendrimers, aiding in the design of dendrimer structures with specific properties. The structure of the Cayley tree can be used to predict how changes in the dendrimer's branching pattern will affect its physical and chemical properties, such as solubility, stability, and reactivity. The Cayley tree provides a framework for simulating the dynamics of dendrimers, including their conformational changes and interactions with other molecules. It is used in theoretical studies to analyze the thermodynamic properties of dendrimers, such as phase transitions and responses to external stimuli. The computed sombor variants are advantageous in predicting physical and chemical properties, material design, synthesis strategy, modeling, and simulation of dendrimers.

5. Conclusion

In this study, we present the edge partition of the banana tree graph. We created sombor indices for them by employing it. Furthermore, we computed Sombor entropies for fractal and cayley tree type dendrimers. With Shannon's equation, the indices that determine the probability function are also utilized to produce other probabilistic entropy measures. The results of this research could significantly advance QSAR and QSPR investigations in the synthesis of dendrimers and novel pharmaceuticals by correlating the defined graphs with several of their physical, chemical, and biological characteristics.

Conflict of interest

The authors declare that they have no conflict of interest.

References

[1] Xue L, Bajorath J. Molecular descriptors in chemoinformatics, computational combinatorial chemistry, and virtual screening. *Combinatorial Chemistry and High Throughput Screening*. 2000; 3(5): 363-372. Available from: https://doi.org/10.2174/1386207003331454.

[2] Todeschini R, Consonni V. *Molecular Descriptors for Chemoinformatics*. New York: John Wiley and Sons; 2009. Available from: https://doi.org/10.1002/9783527628766.

[3] Hong H, Xie Q, Ge W, Qian F, Fang H, Shi L, et al. Mold^2, molecular descriptors from 2D structures for chemoinformatics and toxicoinformatics. *Journal of Chemical Information and Modeling*. 2008; 48(7): 1337-1344. Available from: https://doi.org/10.1021/ci800038f.

[4] Sahoo S, Adhikari C, Kuanar M, Mishra BK. A short review of the generation of molecular descriptors and their applications in quantitative structure property/activity relationships. *Current Computer-Aided Ddrug Desig*. 2016; 12(3): 181-205. Available from: https://doi.org/10.2174/1573409912666160525112114.

[5] Katritzky AR, Gordeeva EV. Traditional topological indexes vs electronic, geometrical, and combined molecular descriptors in QSAR/QSPR research. *Journal of Chemical Information and Computer Sciences*. 1993; 33(6): 835-857. Available from: https://doi.org/10.1021/ci00016a005.

[6] Karelson M. *Molecular Descriptors in QSAR/QSPR*. New York: Wiley-Interscience; 2000.

[7] Varmuza K, Dehmer M, Bonchev D. *Statistical Modelling of Molecular Descriptors in QSAR/QSPR*. New York: Wiley Online Library; 2012. Available from: https://doi.org/10.1002/9783527645121.

[8] Roy K, Kar S, Das RN. *A Primer on QSAR/QSPR Modeling: Fundamental Concepts*. Cham: Springer; 2015. Available from: https://doi.org/10.1007/978-3-319-17281-1.

[9] Bajorath J. Selected concepts and investigations in compound classification, molecular descriptor analysis, and virtual screening. *Journal of Chemical Information and Computer Sciences*. 2001; 41(2): 233-245. Available from: https://doi.org/10.1021/ci0001482.

[10] Trinajstić N. *Chemical Graph Theory*. Boca Raton: CRC Press; 2018. Available from: https://doi.org/10.1201/9781315139111.

[11] Bonchev D. *Chemical Graph Theory: Introduction and Fundamentals*. London: Routledge; 2018.

[12] Gutman I. *Selected Theorems in Chemical Graph Theory*. Kragujevac: University of Kragujevac; 2017.

[13] Estrada E, Patlewicz G, Uriarte E. From molecular graphs to drugs. A review on the use of topological indices in drug design and discovery. *Indian journal of chemistry*. 2003; 42: 1315-1329.

[14] Zanni R, Galvez-Llompart M, Garcia-Domenech R, Galvez J. Latest advances in molecular topology applications for drug discovery. *Expert Opinion on Drug Discovery*. 2015; 10(9): 945-957. Available from: https://doi.org/10.1517/17460441.2015.1062751.

[15] Ivanciuc O. Chemical graphs, molecular matrices and topological indices in chemoinformatics and quantitative structure-activity relationships. *Current Computer-Aided Drug Design*. 2013; 9(2): 153-163. Available from: https://doi.org/10.2174/1573409911309020002.

[16] Redžepović I, Furtula B. Predictive potential of eigenvalue-based topological molecular descriptors. *Journal of Computer-Aided Molecular Design*. 2020; 34(9): 975-982. Available from: https://doi.org/10.1007/s10822-020-00320-2.

[17] Gayathiri V, Manimaran A. Computing certain topological indices of silicate triangle fractal network modeled by the sierpiński triangle network. *Contemporary Mathematics*. 2024; 5(2): 2150-2164. Available from: https://doi.org/10.37256/cm.5220244062.

[18] Redžepović I, Mao Y, Wang Z, Furtula B. Steiner degree distance indices: Chemical applicability and bounds. *International Journal of Quantum Chemistry*. 2020; 120(12): e26209. Available from: https://doi.org/10.1002/qua.26209.

[19] Redžepović I, Furtula B. Resolvent energy and estrada index of benzenoid hydrocarbons. *Journal of the Serbian Society for Computational Mechanics*. 2020; 2020: 37-44. Available from: https://doi.org/10.24874/jsscm.2020.01.04.

[20] Gutman I. Geometric approach to degree-based topological indices: Sombor indices. *MATCH Communications in Mathematical and in Computer Chemistr*. 2021; 86(1): 11-16.

[21] Redžepović I. Chemical applicability of Sombor indices: Survey. *Journal of Serbian Chemical Society*. 2021; 86(5): 445-457. Available from: https://doi.org/10.2298/JSC201215006R.

[22] Das KC, Çevik AS, Cangul IN, Shang Y. On sombor index. *Symmetry*. 2021; 13(1): 140. Available from: https://doi.org/10.3390/sym13010140.

[23] Milovanovic I, Milovanovic E, Matejic M. On some mathematical properties of Sombor indices. *Bulletin of the International Mathematical Virtual Institute*. 2021; 11(2): 341-353. Available from: https://doi.org/10.7251/BIMVI2102341M.

[24] Kulli VR. Different versions of Sombor index of some chemical structures. *International Journal of Engineering Sciences and Research Technology*. 2021; 10(7): 23-32. Available from: http://doi.org/10.29121/ijesrt.v10.i7.2021.4.

[25] Gutman I, Furtula B, Oz MS. Geometric approach to vertex degree based topological indices-Elliptic Sombor index, theory and application. *International Journal of Quantum Chemistry*. 2024; 124(2): e27346. Available from: https://doi.org/10.1002/qua.27346.

[26] Redžepović I. Chemical applicability of Sombor indices. *Journal of the Serbian Chemical Society*. 2021; 86(5): 445-457. Available from: http://doi.org/10.2298/JSC201215006R.

[27] Shanmukha MC, Usha A, Kulli VR, Shilpa KC. Chemical applicability and curvilinear regression models of vertex-degree-based topological index: Elliptic Sombor index. *International Journal of Quantum Chemistry*. 2024; 124(9): e27376. Available from: https://doi.org/10.21203/rs.3.rs-3875265/v2.

[28] Raja NJ, Anuradha A. Topological entropies of single walled carbon nanotubes. *Journal of Mathematical Chemistry*. 2024; 62(4): 809-818. Available from: https://doi-org/10.1007/s10910-023-01532-1.

[29] Hayat S, Arshad M, Khan A. Graphs with given connectivity and their minimum Sombor index having applications to QSPR studies of monocarboxylic acids. *Heliyon*. 2024; 10(1): e23392. Available from: https://doi.org/10.1016/j.heliyon.2023.e23392.

[30] Imran M, Manzoor S, Siddiqui MK, Ahmad S, Muhammad MH. On physical analysis of synthesis strategies and entropy measures of dendrimers. *Arabian Journal of Chemistry*. 2024; 15(2): 103574. Available from: https://doi.org/10.1016/j.arabjc.2021.103574.

[31] Siddiqui MK, Imran M, Iqbal MA. Molecular descriptors of discrete dynamical system in fractal and Cayley tree type dendrimers. *Journal of Applied Mathematics and Computing*. 2019; 61: 57-72. Available from: https://doi.org/10.1007/s12190-019-01238-1.

[32] Rada J, Rodríguez JM, Sigarreta JM. Sombor index and elliptic Sombor index of benzenoid systems. *Applied Mathematics and Computation*. 2024; 475: 128756. Available from: https://doi.org/10.1016/j.amc.2024.128756.

[33] Gutman I, Tošović J. Testing the quality of molecular structure descriptors. Vertex-degree-based topological indices. *Journal of the Serbian Chemical Society*. 2013; 78(6): 805-810. Available from: http://doi.org/10.2298/JSC121002134G.

[34] Buhleier E, Wehner W, Vögtle F. "Cascade" and "nonskid-chain-like" syntheses of molecular cavity topologies. *Synthesis*. 1978; 1978(2): 155-158. Available from: https://doi.org/10.1002/CHIN.197825228.

[35] Klajnert B, Bryszewska M. Dendrimers: Properties and applications. *Acta Biochimica Polonica*. 2001; 48(1): 199-208. Available from: http://doi.org/10.18388/abp.20015127.

[36] Mowshowitz A, Dehmer M. Entropy and the complexity of graphs revisited. *Entropy*. 2012; 14(3): 559-570. Available from: https://doi.org/10.3390/e14030559.

[37] Sabirov DS, Shepelevich IS. Information entropy in chemistry: An overview. *Entropy*. 2021; 23(10): 1240. Available from: https://doi.org/10.3390/e23101240.

[38] Kazemi R. Entropy of weighted graphs with the degree-based topological indices as weights. *MATCH Communications in Mathematical and in Computer Chemistry*. 2016; 76(1): 69-80. Available from: https://doi.org/10.1016/j.arabjc.2020.05.021.

[39] Gayathri P, Priyanka U. Degree based topological indices of banana tree graph. *International Journal of Current Research and Modern Education*. 2017; 2017: 13-24. Available from: https://doi.org/10.5281/zenodo.842195.